

A Bayesian Model for Co-clustering Ordinal Data with Informative Missing Entries

Alice Giampino¹, Antonio Canale², and Bernardo Nipoti¹

¹Department of Economics, Management and Statistics, University of Milano-Bicocca, Piazza
dell'Ateneo Nuovo, 1, Milan, 20126, Italy.

²Department of Statistics, University of Padova, Via C. Battisti, 241, Padova, 35121, Italy.

Abstract

Several approaches have been proposed in the literature for clustering multivariate ordinal data. These methods typically treat missing values as absent information, rather than recognizing them as valuable for profiling population characteristics. To address this gap, we introduce a Bayesian nonparametric model for co-clustering multivariate ordinal data that treats censored observations as informative, rather than merely missing. We demonstrate that this offers a significant improvement in understanding the underlying structure of the data. Our model exploits the flexibility of two independent Dirichlet processes, allowing us to infer potentially distinct subpopulations that characterize the latent structure of both subjects and variables. The ordinal nature of the data is addressed by introducing latent variables, while a matrix factorization specification is adopted to handle the high dimensionality of the data in a parsimonious way. The conjugate structure of the model enables an explicit derivation of the full conditional distributions of all the random variables in the model, which facilitates seamless posterior inference using a Gibbs sampling algorithm. We demonstrate the method's performance through simulations and by analyzing politician and movie ratings data.

1 INTRODUCTION

Multivariate ordinal data, consisting of repeated measurements of vectors of ordinal responses, play a crucial role in various fields. Our focus is on scenarios where repeated measures are available for only a subset of the vector entries, and the missing data can be viewed as informative rather than purely random. For example, in the analysis of political votes, the voting records of n politicians on p legislative bills are only available for the sessions they attended, where absence from a session may represent a deliberate political strategy. Similarly, in recommendation systems, the data consists of customer ratings on p items. In the well-known Netflix Prize data ([Bennett et al.](#),

2007), missingness arises when users choose not to rate certain movies, potentially reflecting their lack of interest, preference, or other underlying factors.

Our analysis of this type of data focuses on clustering both the statistical units and the entries of the ordinal random vectors. This problem can be framed within the context of co-clustering methods (Hartigan, 1972), a set of techniques also known as biclustering or two-mode clustering. The core idea is to simultaneously cluster the rows and columns of an $(n \times p)$ -dimensional data matrix \mathbf{Y} , with rows associated to n statistical units and columns consisting of p ordinal outcomes. Over the past three decades, co-clustering methods have been widely applied across various fields (Busygin et al., 2008), with some approaches resorting to Bayesian nonparametric tools (Meeds and Roweis, 2007; Wang et al., 2011, 2012). Despite extensive literature, most existing methods fail to adequately address the challenges posed by informative missingness. A notable exception is the R package `biclustermd` by Reisner et al. (2019), which uses a geometric approach to optimally rearrange the rows and columns of the data matrix when missing values are present. To our knowledge, no model-based approach for co-clustering with missing entries has yet been explored in the literature. We fill this gap by introducing a flexible Bayesian model capable of performing co-clustering while accounting for the informative nature of missing data. This approach, referred to as the Co-Clustering model for Ordinal Censored Observations (CO^3), employs a latent variable representation to jointly model both the ordinal responses and the indicator variables encoding the presence of missing entries. CO^3 builds on the idea of linking observed discrete data with latent continuous variables, thus following a well-known strategy in Bayesian modeling (Albert and Chib, 1993; Kottas et al., 2005; Canale and Dunson, 2011; Kowal and Canale, 2020). At the level of latent variables, CO^3 employs a Bayesian matrix factorization representation (Salakhutdinov and Mnih, 2008), exploiting the idea that the observed multivariate responses of a statistical unit are driven by a smaller set of unobserved latent factors. Additionally, the definition of CO^3 relies on the flexibility of two independent Dirichlet processes, which allow the model to infer potentially distinct subpopulations characterizing the latent structure of both subjects and variables. This construction not only facilitates the clustering of statistical units and variable entries but also provides a robust framework for effectively addressing the complexities associated with informative censoring. Our investigations show that, while the model is specifically designed to account for informative missingness, its applicability extends to situations where data are missing at random as well.

The rest of the paper is organized as follows. Section 2 is dedicated to the specification of the model. A strategy for posterior computation is presented in Section 3. The performance of the model is investigated by means of the analysis of synthetic and real data, as presented in Sections 4 and 5, respectively. Additional results on the full conditional distributions for posterior sampling, along with further details on the simulation study and the real dataset analyses, are provided in the Supplementary Material.

2 A CO-CLUSTERING MODEL FOR ORDINAL CENSORED OBSERVATIONS

We let $\mathbf{y}_i = (y_{i1}, \dots, y_{ip})$, with $i = 1, \dots, n$, be the i -th row of a data matrix \mathbf{Y} , that is a vector of ordinal responses with the general entry $y_{ij} \in [c]$, for $j = 1, \dots, p$, where $[c] = \{1, \dots, c\}$. For example, in our two motivating applications, y_{ij} represents the vote of the i -th senator in the j -th voting session, or the rating given by i -th user to the j -th movie. In both these applications, as well as in many other contexts, it is common for some components of each observation \mathbf{y}_i to be missing, with the missingness occurring in a non-random manner.

2.1 MODEL FORMULATION

We formalize the missingness by endowing each \mathbf{y}_i with a vector $\boldsymbol{\delta}_i = (\delta_{i1}, \dots, \delta_{ip})$, with δ_{ij} indicating whether the j -th component y_{ij} of \mathbf{y}_i was observed ($\delta_{ij} = 1$) or not ($\delta_{ij} = 0$). This can be easily generalized to the case where, for each unit, there exist q ordinal responses, each accompanied by a corresponding missingness indicator. We will henceforth focus on the specific case with $q = 1$.

Similarly to [Albert and Chib \(1993\)](#) or [Kottas et al. \(2005\)](#), we link both the observed ordinal y_{ij} and the missingness indicators δ_{ij} with latent continuous variables. Specifically, for the ordinal responses, we introduce $\mathbf{z}_i = (z_{i1}, \dots, z_{ip})$ such that

$$\begin{aligned} y_{ij} &= \kappa && \text{if } \gamma_{\kappa-1} < z_{ij} \leq \gamma_{\kappa}; \\ y_{ij} &\in [c] && \text{if } -\infty = \gamma_0 < z_{ij} \leq \gamma_c = \infty. \end{aligned}$$

where $-\infty = \gamma_0 < \gamma_1 < \dots < \gamma_{c-1} < \gamma_c = \infty$ are arbitrarily fixed cutoffs. Similarly, for the censoring variables, we introduce $\mathbf{w}_i = (w_{i1}, \dots, w_{ip})$ such that $\delta_{ij} = 1$ if and only if $w_{ij} \geq 0$. This formulation leads to the following joint distribution for the observed data:

$$\prod_{i,j:\delta_{ij}=1} \Pr(z_{ij} \in (\gamma_{y_{ij}-1}, \gamma_{y_{ij}}]). \quad (1)$$

We now define a Bayesian factor model for the joint distribution of the latent variables $\mathbf{x}_{ij} = (z_{ij}, w_{ij})$. Specifically, we introduce $\boldsymbol{\theta}_{1i}$ and $\boldsymbol{\theta}_{2j}$ to denote the $(d \times 2)$ -dimensional factor matrices for the i -th individual and j -th response, respectively, with $d \ll n, p$. We further model the factor matrices $\boldsymbol{\theta}_{1i}$ and $\boldsymbol{\theta}_{2j}$ with independent Dirichlet processes (DP), leading to

$$\begin{aligned} \mathbf{x}_{ij} &| \boldsymbol{\theta}_1, \boldsymbol{\theta}_2 \stackrel{\text{ind}}{\sim} \text{N}_2(\boldsymbol{\theta}_{1i}^\top \boldsymbol{\theta}_{2j}, \boldsymbol{\Sigma}), && i = 1, \dots, n; j = 1, \dots, p; \\ (\boldsymbol{\theta}_{1i}, \boldsymbol{\theta}_{2j}) &| F_1, F_2 \stackrel{\text{iid}}{\sim} F_1 \times F_2, && i = 1, \dots, n; j = 1, \dots, p; \\ F_l &\stackrel{\text{ind}}{\sim} \text{DP}(\alpha_l, H_l), && l = 1, 2; \end{aligned} \quad (2)$$

where $\boldsymbol{\theta}_1 = \{\boldsymbol{\theta}_{11}, \dots, \boldsymbol{\theta}_{1n}\}$, $\boldsymbol{\theta}_2 = \{\boldsymbol{\theta}_{21}, \dots, \boldsymbol{\theta}_{2p}\}$, $\boldsymbol{\Sigma}$ is a variance-covariance matrix, and α_l and H_l denote, respectively, the concentration parameter and base probability measure of the DP F_l . The

base measures H_l are specified to be matrix normal distributions (see, e.g., [Viroli, 2011](#), for their use in the context of mixture models) with mean matrix \mathbf{M}_l of dimension $d \times 2$ and covariance matrices \mathbf{U}_l and \mathbf{V}_l of dimensions 2×2 and $d \times d$, respectively. We henceforth assume that Σ is diagonal with (σ_1^2, σ_2^2) on the diagonal.

Notably, the introduction of a latent layer of continuous random variables considerably simplifies the task of writing the joint distribution of all the elements in the model, which is the starting point of next section.

2.2 MODEL PROPERTIES

In view of the definition of a MCMC algorithm for posterior inference, described in Section 3, we study the joint conditional distribution of the random elements that constitute the model in (1) and (2), given the data. More specifically, we show the derivation of the conditional distribution that is obtained after marginalizing with respect to the random probability measures F_1 and F_2 . This step conveniently simplifies the task of posterior sampling by analytically integrating out the infinite-dimensional parameters of the model.

We observe that, given the almost sure discreteness of F_1 , the random matrices θ_1 will display ties with positive probability and thus the set θ_1 can be equivalently described in terms of $k_n \leq n$ distinct values $\theta_{1\ell_1}^*$, with $\ell_1 = 1, \dots, k_n$, and their frequency $n_{\ell_1} = \sum_{i=1}^n \delta_{\theta_{1\ell_1}^*}(\theta_{1i})$ in θ_1 . Similarly, θ_2 can be described by $k_p \leq p$ distinct values $\theta_{2\ell_2}^*$, with $\ell_2 = 1, \dots, k_p$, and their frequency $n_{\ell_2} = \sum_{j=1}^p \delta_{\theta_{2\ell_2}^*}(\theta_{2j})$ in θ_2 . As a result, using independent Dirichlet processes to model θ_1 and θ_2 conveniently facilitates the simultaneous clustering of subjects and responses. This is particularly relevant in our motivating political application, where analysts are interested in grouping politicians based on their actual voting behaviors and in determining whether this alignment corresponds with their party affiliations. At the same time, this approach can help in categorizing voting sessions to identify patterns in legislative priorities and uncover strategic collaborations across party lines. The distributions of (n_1, \dots, n_{k_n}) and (p_1, \dots, p_{k_p}) are characterized by the exchangeable partition probability function (EPPF) of the DP, for which we have

$$\Pi_{k_n}^{(n)}(n_1, \dots, n_{k_n}) = \frac{\alpha_1^{k_n}}{(\alpha_1)_n} \prod_{\ell_1=1}^{k_n} (n_{\ell_1} - 1)!, \quad \Pi_{k_p}^{(p)}(p_1, \dots, p_{k_p}) = \frac{\alpha_2^{k_p}}{(\alpha_2)_p} \prod_{\ell_2=1}^{k_p} (p_{\ell_2} - 1)!,$$

where the symbol $(a)_n = a(a+1) \cdots (a+n-1)$ is used to denote the ascending factorial. To be more specific, $\Pi_{k_n}^{(n)}(n_1, \dots, n_{k_n})$ gives the probability of observing any specific partition of the elements of θ_1 in k_n distinct values of cardinality $\{n_1, \dots, n_{k_n}\}$; similarly for $\Pi_{k_p}^{(p)}(p_1, \dots, p_{k_p})$.

We introduce $\theta = \{\theta_1, \theta_2\}$ and \mathbf{X} to be the tensor with n rows, p columns, and 2 tubes, containing in row i , column j , the vector \mathbf{x}_{ij} and we focus on studying the conditional distribution $p(\theta, \mathbf{X} \mid \mathcal{D})$ of the latent variables $\{\theta, \mathbf{X}\}$, given the data \mathcal{D} . Here and henceforth, $p(\cdot)$ denotes the distribution of a generic random element. Marginalizing the distribution implied by (1) and

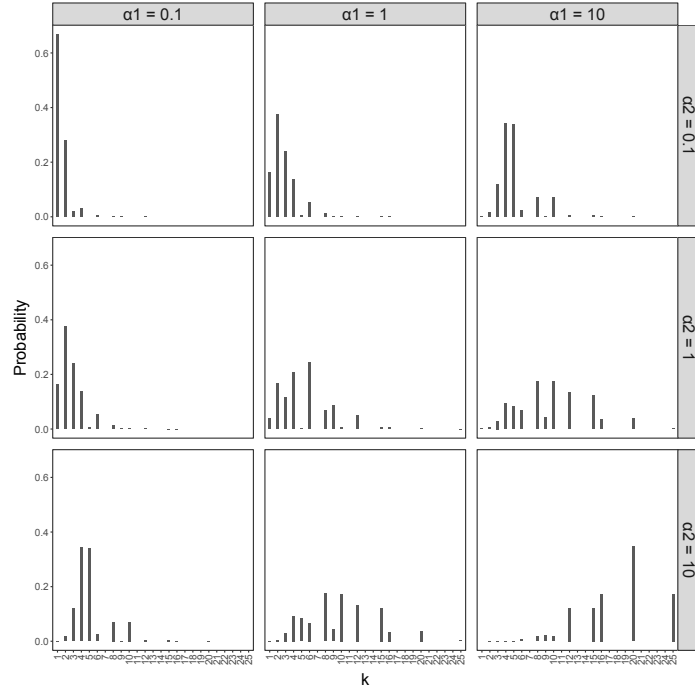


Figure 1: Prior distribution of the number of bivariate clusters k in CO^3 , for $n = p = 5$, and different values of α_1 and α_2 ranging in $\{0.1, 1, 10\}$.

(2) with respect to the DPs F_1 and F_2 , we get

$$\begin{aligned}
 p(\boldsymbol{\theta}, \mathbf{X} \mid \mathcal{D}) &\propto \Pi_{k_n}^{(n)}(n_1, \dots, n_{k_n}) \Pi_{k_p}^{(p)}(p_1, \dots, p_{k_p}) \prod_{\ell_1=1}^{k_n} h_1(\boldsymbol{\theta}_{1\ell_1}^*) \prod_{\ell_2=1}^{k_p} h_2(\boldsymbol{\theta}_{2\ell_2}^*) \\
 &\times \prod_{i \in \mathcal{C}_{1\ell_1}} \prod_{j \in \mathcal{C}_{2\ell_2}} p(y_{ij}, \delta_{ij} \mid \mathbf{x}_{ij}) p(\mathbf{x}_{ij} \mid \boldsymbol{\theta}_{1\ell_1}^*, \boldsymbol{\theta}_{2\ell_2}^*), \tag{3}
 \end{aligned}$$

where h_l denotes the probability density function corresponding to the base measure H_l , for $l = 1, 2$, and $\mathcal{C}_{1\ell_1} = \{i \in \{1, \dots, n\} : \boldsymbol{\theta}_{1i} = \boldsymbol{\theta}_{1\ell_1}^*\}$ and $\mathcal{C}_{2\ell_2} = \{j \in \{1, \dots, p\} : \boldsymbol{\theta}_{2j} = \boldsymbol{\theta}_{2\ell_2}^*\}$. From (3) one can obtain the full conditional distributions of the elements of $\boldsymbol{\theta}$ and \mathbf{X} .

Given the focus is on simultaneously clustering of subjects and responses, it is interesting to study the prior properties of $k = k_n k_p$, which we refer to as the number of bivariate clusters and which corresponds to the cardinality of the set of all possible pairs of cluster assignments $\{(\ell_1, \ell_2) : \ell_1 = 1, \dots, k_n \text{ and } \ell_2 = 1, \dots, k_p\}$. The independence of F_1 and F_2 facilitates the task, and we get that k has distribution

$$\Pr(k = \ell) = \frac{1}{(\alpha_1)_n (\alpha_2)_p} \sum_{i,j:ij=\ell} \alpha_1^i \alpha_2^j |s(n, i)| |s(p, j)|,$$

where $s(n, i)$ is the Stirling number of the first type. As an example, Figure 1 displays the prior distribution of the number of bivariate clusters k when $n = p = 5$ and for different values of the concentration parameters α_1 and α_2 . As the latter ones increase, the distribution of k concentrates

on larger values. Consistently with this, the expected value of k is

$$\mathbb{E}[k] = \alpha_1 \alpha_2 \sum_{i=1}^n \frac{1}{\alpha_1 + i - 1} \sum_{j=1}^p \frac{1}{\alpha_2 + j - 1}. \quad (4)$$

Finally, we observe that, as both n and p grow to infinity, the number of bivariate clusters grows proportionally to $\log(n) \log(p)$. Specifically, we have

$$\frac{k}{\log(n) \log(p)} \longrightarrow \alpha_1 \alpha_2 \text{ almost surely,}$$

as $n, p \longrightarrow \infty$.

3 POSTERIOR COMPUTATION

Equation (3) provides the starting point to devise a Gibbs sampler for posterior inference. The update of the parameters is conveniently facilitated by the availability of closed-form full conditional distributions, which we discuss for the random elements of model (1) and (2), namely $\mathbf{z}_i, \mathbf{w}_i, \boldsymbol{\theta}_{1i}, \boldsymbol{\theta}_{2i}, \sigma_1^2, \sigma_2^2$. To this end, we introduce additional notation. For any $r = 1, 2$, we denote the r -th column of $\boldsymbol{\theta}_{1i}$ and $\boldsymbol{\theta}_{2j}$ as $\boldsymbol{\theta}_{1i}^{(r)}$ and $\boldsymbol{\theta}_{2j}^{(r)}$, respectively. Moreover, we introduce the $(d \times n)$ -dimensional matrix $\boldsymbol{\theta}_1^{(r)}$ as the matrix whose i -th column coincides with $\boldsymbol{\theta}_{1i}^{(r)}$, and the $(d \times p)$ -dimensional matrix $\boldsymbol{\theta}_2^{(r)}$ as the matrix whose j -th column coincides with $\boldsymbol{\theta}_{2j}^{(r)}$.

The full conditional distributions of \mathbf{z}_i and \mathbf{w}_i are p -dimensional truncated multivariate normal distributions with independent components. This implies that, for any $j = 1, \dots, p$,

$$z_{ij} \mid \dots \stackrel{\text{ind}}{\sim} \delta_{ij} \text{TN} \left(\boldsymbol{\theta}_{2j}^{(1)\top} \boldsymbol{\theta}_{1i}^{(1)}, \sigma_1^2; \gamma_{y_{ij}-1}, \gamma_{y_{ij}} \right) + (1 - \delta_{ij}) \text{N} \left(\boldsymbol{\theta}_{2j}^{(1)\top} \boldsymbol{\theta}_{1i}^{(1)}, \sigma_1^2 \right), \quad (5)$$

where $\text{TN}(m, s^2; a, b)$ is used to denote a two-sided truncated normal with mean m , variance s^2 and support (a, b) . Similarly,

$$w_{ij} \mid \dots \stackrel{\text{ind}}{\sim} \delta_{ij} \text{TN} \left(\boldsymbol{\theta}_{2j}^{(2)\top} \boldsymbol{\theta}_{1i}^{(2)}, \sigma_2^2; 0, \infty \right) + (1 - \delta_{ij}) \text{TN} \left(\boldsymbol{\theta}_{2j}^{(2)\top} \boldsymbol{\theta}_{1i}^{(2)}, \sigma_2^2; -\infty, 0 \right). \quad (6)$$

Next, we observe that, conditionally on the continuous latent vectors \mathbf{z}_i and \mathbf{w}_i , the random vectors $\boldsymbol{\theta}_{1i}$ and $\boldsymbol{\theta}_{2i}$ are independent of the observations \mathbf{y}_i and $\boldsymbol{\delta}_i$. Their distribution is governed by model (2), which incorporates two independent DPs. The literature on computational methods for DP-based models, or other discrete nonparametric priors, is extensive, providing various strategies to handle the infinite dimensionality of such models. Examples include [Escobar and West \(1995\)](#), [Papaspiliopoulos and Roberts \(2008\)](#), [Kalli et al. \(2011\)](#), and [Canale et al. \(2022\)](#). In this work, we adapt the marginal approach of [Escobar and West \(1995\)](#) to accommodate the additional complexity introduced by the two DPs in our model. Specifically, the marginalization of model (2) with respect to F_1 and F_2 , yields full conditional distributions for $\boldsymbol{\theta}_{1i} = (\boldsymbol{\theta}_{1i}^{(1)}, \boldsymbol{\theta}_{1i}^{(2)})$ and $\boldsymbol{\theta}_{2j} = (\boldsymbol{\theta}_{2j}^{(1)}, \boldsymbol{\theta}_{2j}^{(2)})$ whose form is reminiscent of the generalized Pólya urn scheme ([Blackwell and MacQueen, 1973](#)).

Namely,

$$\Pr(\boldsymbol{\theta}_{1i} \in d\mathbf{t} \mid \dots) = \pi_{1i0} G_{1i}(d\mathbf{t}) + \sum_{\ell=1}^{k_{n(i)}} \pi_{1i\ell} \delta_{\boldsymbol{\theta}_{1\ell(i)}^*}(\mathbf{t}) \quad i = 1, \dots, n \quad (7)$$

$$\Pr(\boldsymbol{\theta}_{2j} \in d\mathbf{t} \mid \dots) = \pi_{2j0} G_{2j}(d\mathbf{t}) + \sum_{\ell=1}^{k_{p(j)}} \pi_{2j\ell} \delta_{\boldsymbol{\theta}_{2\ell(j)}^*}(\mathbf{t}) \quad j = 1, \dots, p \quad (8)$$

where the subscript (i) (or (j)) is used to denote quantities that are computed after excluding the element $\boldsymbol{\theta}_{1i}$ from $\boldsymbol{\theta}_1$ (or $\boldsymbol{\theta}_{2j}$ from $\boldsymbol{\theta}_2$). The weights $\{\pi_{1i0}, \dots, \pi_{1ik_{n(i)}}\}$ in (7) and $\{\pi_{2j0}, \dots, \pi_{2jk_{p(j)}}\}$ in (8), provided in the Supplementary Material, are available in closed form. The distributions G_{1i} in (7) and G_{2j} in (8) are easy to sample from as they can be written as a conditional chain of d -dimensional normal distributions, as described in the Supplementary Material. A convenient simplification that will be implemented for the analyses of Sections 4 and 5 is achieved by assuming that the base measures H_l are characterized by independence between columns. This is equivalent to assuming that the column covariance matrices \mathbf{U}_l are diagonal, which allows us to decompose the matrix variate normal base measure into a product of independent multivariate normal distributions. As a result, the form of the weights π_{1i0} and π_{2j0} simplifies considerably, and the problem of sampling from G_{1i} and G_{2j} reduces to sampling from independent d -dimensional normal distributions. Again, details are deferred to the Supplementary Material.

It is well known that algorithms based on Pólya urn schemes can suffer of slow mixing (see, e.g., the discussion in [Ishwaran and James, 2001](#)). A solution to deal with this problem is the introduction of a reshuffling step to update the distinct values of the latent variables from their full conditional distributions. We observe that

$$\begin{aligned} \Pr(\boldsymbol{\theta}_{1\ell_1}^* \in (d\mathbf{t}_1, d\mathbf{t}_2) \mid \dots) &\propto H_1(d\mathbf{t}_1, d\mathbf{t}_2) \\ &\times \exp \left\{ -\frac{1}{2} \text{tr} \left[\frac{1}{\sigma_1^2} \sum_{i \in \mathcal{C}_{\ell_1}} (\mathbf{z}_i - \boldsymbol{\theta}_2^{(1)\top} \mathbf{t}_1)(\mathbf{z}_i - \boldsymbol{\theta}_2^{(1)\top} \mathbf{t}_1)^\top \right] \right\} \\ &\times \exp \left\{ -\frac{1}{2} \text{tr} \left[\frac{1}{\sigma_2^2} (\mathbf{w}_i - \boldsymbol{\theta}_2^{(2)\top} \mathbf{t}_2)(\mathbf{w}_i - \boldsymbol{\theta}_2^{(2)\top} \mathbf{t}_2)^\top \right] \right\}, \end{aligned} \quad (9)$$

for any $\ell_1 = 1, \dots, k_n$, and that, similarly,

$$\begin{aligned} \Pr(\boldsymbol{\theta}_{2\ell_2}^* \in (d\mathbf{s}_1, d\mathbf{s}_2) \mid \dots) &\propto H_2(d\mathbf{s}_1, d\mathbf{s}_2) \\ &\times \exp \left\{ -\frac{1}{2} \text{tr} \left[\frac{1}{\sigma_1^2} \sum_{j \in \mathcal{C}_{\ell_2}} (\mathbf{z}_j - \boldsymbol{\theta}_1^{(1)\top} \mathbf{s}_1)(\mathbf{z}_j - \boldsymbol{\theta}_1^{(1)\top} \mathbf{s}_1)^\top \right] \right\} \\ &\times \exp \left\{ -\frac{1}{2} \text{tr} \left[\frac{1}{\sigma_2^2} (\mathbf{w}_j - \boldsymbol{\theta}_1^{(2)\top} \mathbf{s}_2)(\mathbf{w}_j - \boldsymbol{\theta}_1^{(2)\top} \mathbf{s}_2)^\top \right] \right\}, \end{aligned} \quad (10)$$

for any $\ell_2 = 1, \dots, k_p$. As already observed for the distributions G_{1i} and G_{2j} , also the distributions in (9) and (10) can be written as a conditional chain of d -dimensional normal distributions. Moreover, under the additional assumption that the column covariance matrices \mathbf{U}_l are diagonal, one gets that the columns of $\boldsymbol{\theta}_{1\ell_1}^*$ distributed as (9), and similarly those of $\boldsymbol{\theta}_{1\ell_1}^*$ distributed as in (10), are independent d -dimensional normal random vectors, with parameters reported in the

Supplementary Material.

Finally, if the model is completed by specifying Inverse-gamma hyperpriors for the σ_1^2 and σ_2^2 , namely $\sigma_l^2 \sim \text{IG}(\alpha_{\sigma_l}, \beta_{\sigma_l})$ with $l = 1, 2$, then, the full conditionals for σ_1^2 and σ_2^2 are given by

$$\sigma_1^2 \mid \dots \sim \text{IG} \left(\alpha_{\sigma_1} + \frac{np}{2}, \beta_{\sigma_1} + \frac{1}{2} \sum_{i=1}^n \sum_{j=1}^p (z_{ij} - \boldsymbol{\theta}_{1i}^{(1)\top} \boldsymbol{\theta}_{2j}^{(1)})^2 \right), \quad (11)$$

$$\sigma_2^2 \mid \dots \sim \text{IG} \left(\alpha_{\sigma_2} + \frac{np}{2}, \beta_{\sigma_2} + \frac{1}{2} \sum_{i=1}^n \sum_{j=1}^p (w_{ij} - \boldsymbol{\theta}_{1i}^{(2)\top} \boldsymbol{\theta}_{2j}^{(2)})^2 \right). \quad (12)$$

Algorithm 1 outlines the steps of the Gibbs sampler we obtain by combining the sequential updates of the model parameters according to the corresponding full conditional distributions, with the reshuffling step. Extending the algorithm to the case of $2q$ response variables poses no significant challenges, as the additional latent factor vectors corresponding to the continuous latent variables are jointly handled within the two Pólya urn steps of the algorithm. Finally, we note that throughout this work, the rows and the columns of the data matrix \mathbf{Y} are partitioned, based on the posterior output produced by Algorithm 1, by resorting to Variation of Information with complete linkage (Wade and Ghahramani, 2018).

Algorithm 1 Gibbs sampling for CO^3

```

1: set admissible initial values for the latent vectors  $\boldsymbol{\theta}_1$  and  $\boldsymbol{\theta}_2$ 
2: for each iteration  $b = 1 \dots, B$  do:
3:   for each  $i = 1, \dots, n$  and  $j = 1, \dots, p$  do: ▷ generalized Pólya urns
4:     sample  $\boldsymbol{\theta}_{1i}$  from Equation 7
5:     sample  $\boldsymbol{\theta}_{2j}$  from Equation 8
6:   set  $\boldsymbol{\theta}_1^* = (\boldsymbol{\theta}_{11}, \dots, \boldsymbol{\theta}_{1k_n})$  be the vector of distinct parameters in  $\boldsymbol{\theta}_1$ .
7:   set  $\boldsymbol{\theta}_2^* = (\boldsymbol{\theta}_{21}, \dots, \boldsymbol{\theta}_{2k_p})$  be the vector of distinct parameters in  $\boldsymbol{\theta}_2$ .
8:   for each  $\ell_1 = 1, \dots, k_n$  do: ▷ reshuffling step 1
9:     let  $C_{\ell_1}$  be the set of indexes  $i$  such that  $\boldsymbol{\theta}_{1i} = \boldsymbol{\theta}_{1\ell_1}^*$ ;
10:    sample  $\boldsymbol{\theta}_{1\ell_1}^*$  from Equation 9
11:  for each  $\ell_2 = 1, \dots, k_p$  do: ▷ reshuffling step 2
12:    let  $C_{\ell_2}$  be the set of indexes  $j$  such that  $\boldsymbol{\theta}_{2j} = \boldsymbol{\theta}_{2\ell_2}^*$ ;
13:    sample  $\boldsymbol{\theta}_{2\ell_2}^*$  from Equation 10
14:  for each  $i = 1, \dots, n$  and  $j = 1, \dots, p$  do: ▷ update of continuous latent variables
15:    sample  $z_{ij}$  from Equation 5
16:    sample  $w_{ij}$  from Equation 6
17:  sample  $\sigma_1^2$  from Equation 11 ▷ update of hyperparameters
18:  sample  $\sigma_2^2$  from Equation 12
19: end

```

A key step in implementing the CO^3 model involves specifying the latent dimension d . A suitable choice of d should strike a balance: on the one hand, a smaller d is appealing as it keeps computations tractable and favours the interpretability of the analysis results. On the other hand, d needs to be large enough to capture and distinguish the key features of the p -dimensional observations, even when projected onto a d -dimensional space, with $d \ll p$. We propose selecting d on a case-by-case basis by comparing the predictive performance of models with different values of d . This will be

done by evaluating the Log Pseudo Marginal Likelihood (LPML) (Geisser and Eddy, 1979) for a range of values of d . Our approach offers two main advantages: first, we keep the latent variables dimension fixed when implementing Algorithm 1, thus avoiding the issue of dealing with trans-dimensional steps; second, it provides useful insights into how the choice of d affects the model’s predictive ability. Other strategies are possible and have been explored in recent literature. A notable approach, which has gained considerable attention in factor models, involves the use of shrinkage priors (Bhattacharya and Dunson, 2011; Legramanti et al., 2020). These priors for d have support on the set of positive integers and promote sparsity by inducing posterior shrinkage towards smaller dimensions.

4 SIMULATION STUDIES

We assess the performance of CO^3 in co-clustering individuals and items using synthetic data generated across various scenarios, differing in dimensionality and characterised by censoring mechanisms of varying intensity and nature. In each scenario, data are simulated under the correct model specification, specifically by generating the latent variables \mathbf{x}_{ij} according to the first equation in (2). The study is organized in two parts. In both, we assess the co-clustering performance of CO^3 and we compare it against that one of the `biclustermd` R package. CO^3 is implemented by running Algorithm 1 for 5,000 iterations, with the first half discarded as burn-in. For simplicity, rather than assigning hyperpriors as in (11) and (12), we set $\sigma_1^2 = 0.1$ and $\sigma_2^2 = 1.5$. The concentration parameters α_1 and α_2 of F_1 and F_2 are both fixed equal to 1. Additionally, for $l = 1, 2$, we set $u_{l11} = u_{l22} = 1/\sqrt{d}$, where u_{l11} and u_{l22} are the entries of the diagonal matrix \mathbf{U}_l , and \mathbf{M}_l is defined as a matrix of zeros. While CO^3 infers the number of clusters for both rows and columns of \mathbf{Y} , for `biclustermd` we set the number of clusters to match the actual numbers used in data simulation, thus facilitating row and column clustering for this alternative approach.

In the first part of this study, ordinal observations are generated to resemble the movie ratings data analysed in Section 5.2. Specifically, we assume that the ratings \mathbf{y}_i take values in $\{1, 2, 3\}$ and consider a scenario characterised by three types of users and three types of movies. To achieve this, the matrices $\boldsymbol{\theta}_{1i}$ and $\boldsymbol{\theta}_{2j}$ are randomly generated from mixtures with three components each. Additionally, we censor 5% of the observations, randomly selected from records corresponding to the lowest ratings, thereby simulating a mechanism where missing entries may indicate a lack of interest in specific movies. We henceforth refer to this mechanism as informative censoring. Data are generated with different values for n and p , with $(n, p) \in \{(50, 50), (100, 100), (200, 200)\}$. For each scenario, 100 independent datasets are generated. An example is provided in Figure B1 in the Supplementary Material.

In order to select d , we ran the model on a single dataset, selected at random from the 100 replicates with $n = p = 50$ and 5% censored observations, for different specifications of $d \in \{2, \dots, 20\}$. The LPML plot, shown in the left panel of Figure 2, suggests that $d = 3$ is optimal, and this value is fixed for all subsequent analyses.

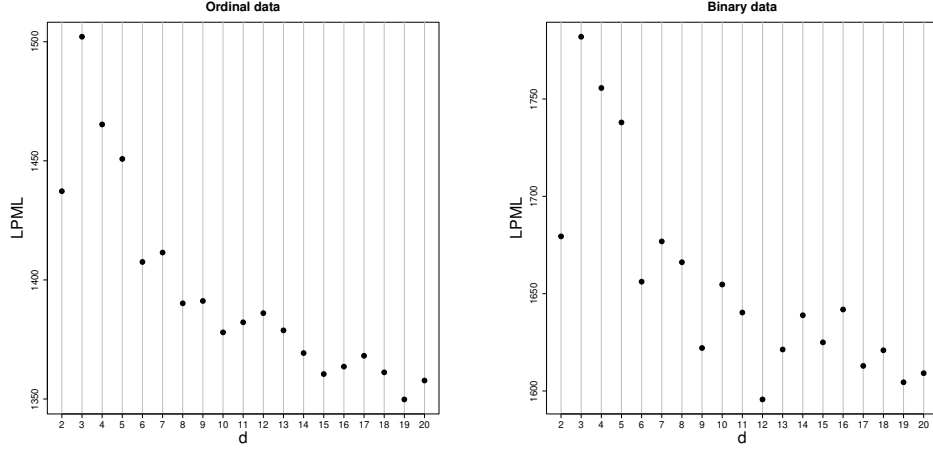


Figure 2: Simulated data with informative censoring. LPML for different values of the latent dimension d on a randomly selected dataset with $n = p = 50$ and 5% of informative censoring, with ordinal observations (left panel) and binary observations (right panel).

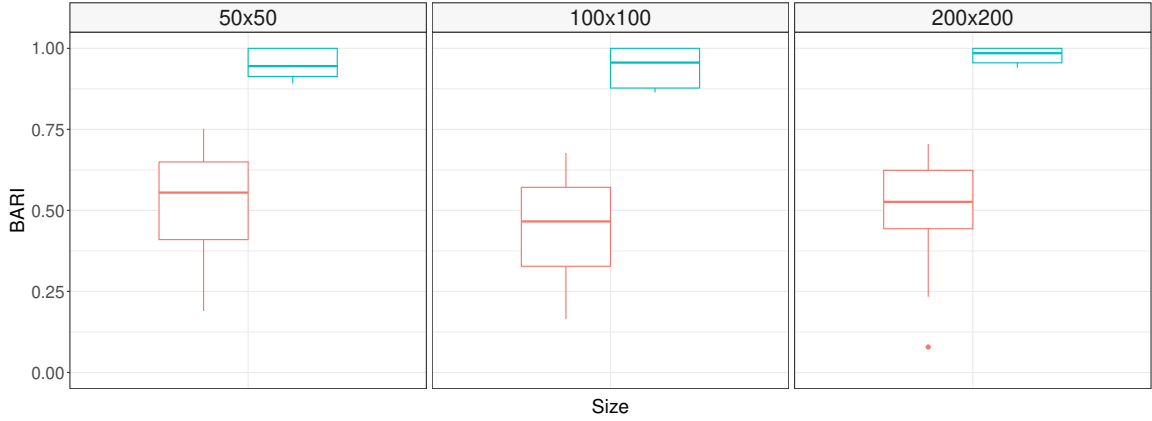


Figure 3: Simulated ordinal data with informative censoring. Boxplot for the BARI comparing the true bivariate partition and those identified by `biclustermmd` (left boxplots) and `CO3` (right boxplots), for different data size.

Given the bivariate nature of the co-clustering problem, the performance of a method is assessed using a bivariate extension of the Adjusted Rand Index (ARI, [Rand, 1971](#)), referred to as the bivariate ARI (BARI), to compare true and estimated partitions. The BARI provides a summary measure of a model’s ability to correctly cluster both rows and columns of a data matrix. Specifically, when analysing the data matrix \mathbf{Y} , the BARI is defined as the ARI between the estimated and true partition of the np data entries $\{y_{ij} : i = 1, \dots, n \text{ and } j = 1, \dots, p\}$, where $y_{i_1 j_1}$ and $y_{i_2 j_2}$, with $(i_1, j_1) \neq (i_2, j_2)$, are in the same cluster if and only if the i_1 -th and i_2 -th rows belong to the same cluster, and the j_1 -th and j_2 -th columns belong to the same cluster, according to the marginal partitions of rows and columns. The results of our study are presented in [Figure 3](#), showing that `CO3` consistently outperforms `biclustermmd`. The performance of `CO3` appears rather stable performance across varying dataset sizes, with the median BARI increasing slightly as dataset size grows, indicating that larger datasets favour the recovery of true latent clusters. In

contrast, `biclustermd` yields BARI values consistently around 50%. We also evaluated `CO3`'s ability to estimate the marginal partitions for the rows and columns of \mathbf{Y} . The results of our analysis, summarized in Table B1 in the Supplementary Material, confirm `CO3`'s robust performance across different dataset sizes.

We now turn to the second part of the simulation study, which investigates how `CO3` performs when analyzing datasets characterized by different types of censoring mechanisms, and how it compares to `biclustermd`. In this experiment, the data dimensions are fixed at $n = p = 50$. The data are simulated to mimic the voting patterns of politicians, which will be discussed in Section 5.1. In this context, we assume that observations y_{ij} take values in $\{0, 1\}$, representing votes {no, yes} on a specific political query. We reproduce a scenario with three major political parties and three types of voting patterns, achieved by simulating θ_{1i} and θ_{2j} from three-component mixture models. A portion of the observations, specifically 5% or 15%, is censored under two different schemes: (i) randomly, referred to as “non-informative censoring”, and (ii) uniformly at random among the entries equal to 0, termed “informative censoring”. The latter simulates a mechanism where missing entries may indicate opposition to a political motion. For each scenario, 100 independent datasets are generated. Examples of datasets simulated under this framework are illustrated in Figures B2 in the Supplementary Material. Also for this second experiment, the latent dimension d was determined using the LPML criterion. The right panel of Figure 2 indicates that $d = 3$ is the optimal choice in this scenario as well.

The results of the experiment, displayed in Figure 4, confirm the findings from the first part of the study, indicating that `CO3` outperforms `biclustermd` across all scenarios, with consistently larger values for the BARI. Notably, `CO3` excels in scenarios involving informative censoring, demonstrating its ability to exploit this additional source of information. Nevertheless, its performance remains robust even in scenarios where the censoring mechanism characterizing the data-generating process is non-informative. Overall, and as expected, the true latent clusters are identified more accurately in settings with 5% censorship compared to those with 15%.

5 REAL DATA ILLUSTRATIONS

We demonstrate the functionality of `CO3` by analyzing two real-world datasets. The first dataset contains votes from U.S. senators and is characterized by binary responses, as discussed in one of the simulation studies in Section 4. The second dataset relates to movie rankings, which are characterized by ordinal responses, as explored in the other simulation study in Section 4. For both analyses, the hyperparameters are specified as outlined in Section 4, with the exception of the DPs' concentration parameters, which are set equal to $\alpha_1 = 10^{-5}$ and $\alpha_2 = 10^5$, respectively, to favor robust inference.

5.1 U.S. SENATORS DATA

Political data offer valuable insights into voting behavior within parties, revealing, for example, whether politicians consistently follow party lines or show divergent voting patterns. The dataset

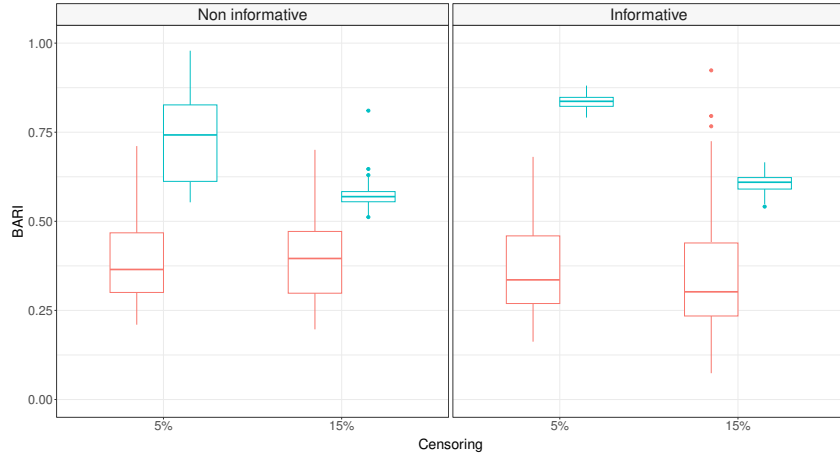


Figure 4: Simulated binary data. Boxplots for the BARI comparing the true bivariate partition and those identified by `biclustermd` (left boxplots) and `CO3` (right boxplots). This comparison is made for datasets with 5% or 15% of entries missing, generated by a non-informative censoring mechanism (left panel) or an informative one (right panel).

we consider was retrieved from [voteview.com](#) (Boche et al., 2018) and it includes the voting records of 100 U.S. senators across 35 voting sessions held between May 2, 2022, and May 16, 2022. Notably, 3.37% of the data entries are missing, corresponding to instances where a senator did not participate in a given session. It is reasonable to assume that censored observations hold valuable information, given that the choice to abstain from voting in a particular session is frequently a political statement in its own right. As for the simulated data considered in Section 4, we resort to the LPML to set the value of the latent dimension d . Our analysis suggests that the best predictive performance is achieved when setting $d = 3$. See Figure C3 in the Supplementary Material for details.

The results of our analysis, summarized by the alluvial diagrams in Figure 5, offer valuable insights by comparing the identified clusters with available information on voting session types and party affiliations. For instance, voting sessions can be categorized into nominations to appoint someone to a specific position, motions, and resolutions. Our analysis identifies one large cluster containing nearly all the nominations and just over half of the motions, and a smaller cluster dominated by motions and resolutions. This outcome suggests potential similarities in the way senators voted on particular motions and nominations. Specifically, the cluster labeled 1 in the top panel of Figure 5 mainly consists of motions and nominations related to appointing individuals to specific roles, while cluster 2 in the same plot is primarily composed of motions on bills supporting federal research initiatives to maintain U.S. leadership in engineering biology and resolutions addressing various health policy changes. At the same time, examining the marginal results for the Senators, shown in the bottom panel of Figure 5, reveals a significant polarization along party lines. Notably, independent senators are grouped with their Democratic counterparts. Additionally, a smaller third cluster indicates that the votes of nine Republican senators align with those of five Democratic senators. The names of these senators are listed in Table C2 in the Supplementary Material: the composition of this third cluster may offer valuable insights for analysts studying U.S. parliamentary dynamics.

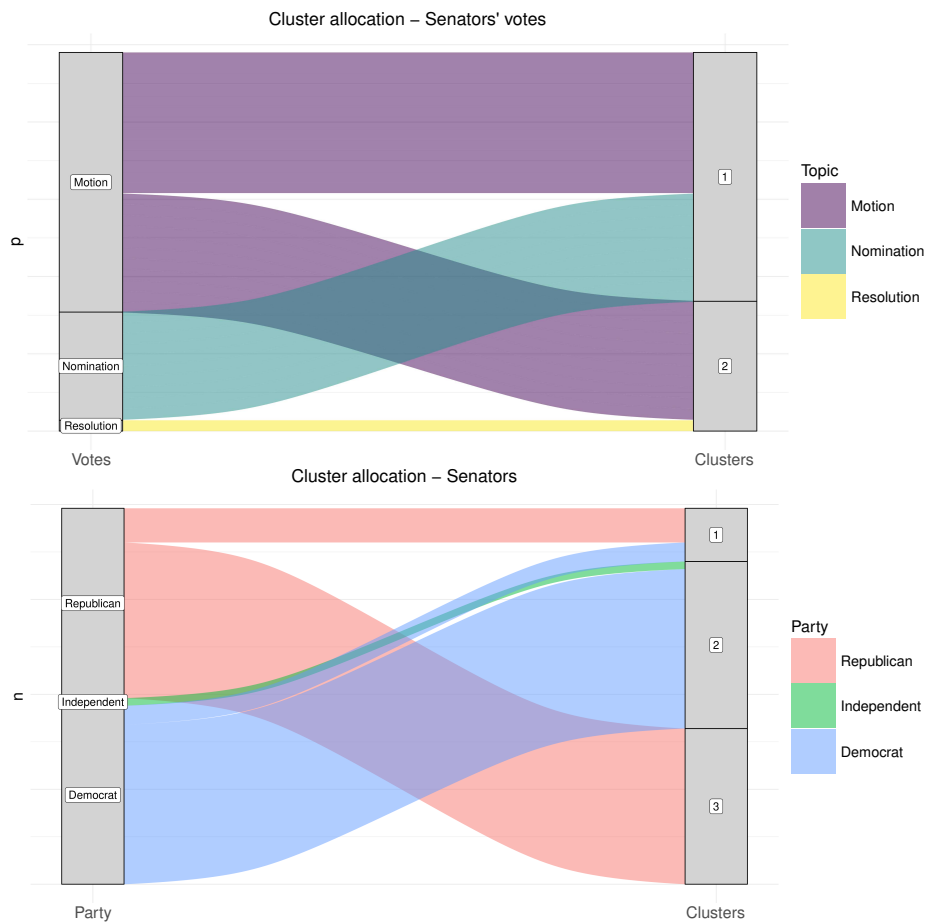


Figure 5: U.S. Senators Data. Alluvial diagrams comparing the estimated marginal clusters of votes (upper panel) and senators (lower panel). On the left of the plots, we report the topic of voting sessions (upper panel) and party affiliation (lower panel).

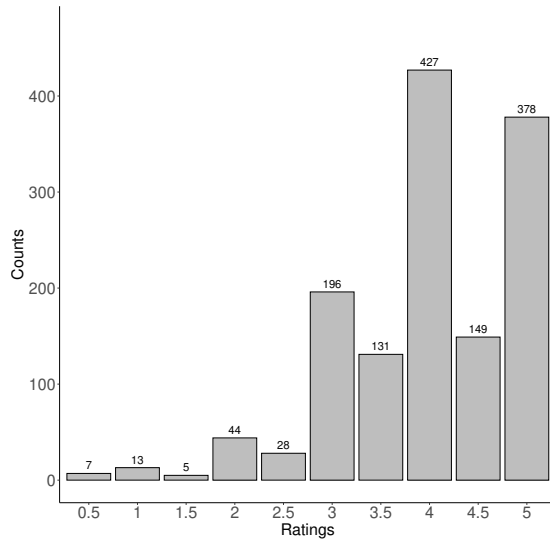


Figure 6: Movielens Data. Empirical frequencies of the movie ratings.

5.2 MOVIELENS DATA

As a second illustrative application, we analyze a portion of the Movielens dataset, available in the R package `ds1labs` (Irizarry and Gill, 2021), which includes data from 60 users and 28 movies, and for which 17.98% of the entries are missing. The ratings range from $\{0.5, 1, \dots, 5\}$, with Figure 6 displaying the corresponding frequencies. The distribution of ratings is heavily concentrated around values of 3 and above, likely due to the dataset consisting of well-known and critically acclaimed movies. Additionally, the frequencies for half-point ratings, such as $\{0.5, 1.5, 2.5, 3.5, 4.5\}$, are lower than those for whole-number ratings, which include $\{1, 2, 3, 4, 5\}$. As with the other datasets in this work, the latent dimension d was selected by running the analysis with different values of d and evaluating the corresponding LPML. This analysis indicated that $d = 2$ is optimal, as shown in Figure C4 in the Supplementary Material.

The results reveal four distinct groups of movies, henceforth labeled as clusters 1, 2, 3, and 4 for convenience. A closer examination of these groups shows that they are well differentiated by the genres of the movies they contain. Cluster 1 represents the genre “Drama/Thriller”, with the only surprising inclusion being “Toy Story”, which, based on its tags, seems an unexpected fit for this cluster. Cluster 2 comprises “Adventure/Action” movies and exhibits a rather homogeneous composition. The movies in Cluster 3 are characterized by plots involving a journey that the characters undertake to resolve their misadventures. In contrast, Cluster 4, which also appears rather homogeneous, consists of more satirical movies. Table 1 lists the titles of the 28 movies in the dataset, along with their genres and cluster allocations.

The estimated partition of the 60 users in the dataset reveals six clusters with frequencies of $\{8, 31, 4, 7, 9, 1\}$, which we will refer to as Clusters 1, 2, 3, 4, 5, and 6 for convenience. To protect user privacy, no individual information was provided in the original dataset. Therefore, to gain insights into the composition of each user cluster, we analyze how users in each group rated movies across the four movie clusters: “Drama/Thriller”, “Adventure/Action”, “Journey”, and “Satire”.

Title	Genre	Cluster
“Seven”	Mystery Thriller	1
“Pulp Fiction”	Comedy Crime Drama Thriller	1
“The Silence of the Lambs”	Crime Horror Thriller	1
“The Shawshank Redemption”	Crime Drama	1
“The Sixth Sense”	Drama Horror Mystery	1
“American Beauty”	Drama Romance	1
“The Godfather”	Crime Drama	1
“The Matrix”	Action Sci-Fi Thriller	1
“Toy Story”	Adventure Animation Children Comedy Fantasy	1
“Braveheart”	Action Drama War	2
“Forrest Gump”	Comedy Drama Romance War	2
“Speed”	Action Romance Thriller	2
“Jurassic Park”	Action Adventure Sci-Fi Thriller	2
“Star Wars: Ep. VI”	Action Adventure Sci-Fi	2
“Men in Black”	Action Comedy Sci-Fi	2
“Star Wars: Ep. IV”	Action Adventure Sci-Fi	2
“Die Hard”	Action Crime Thriller	2
“Star Wars: Ep. V”	Action Adventure Sci-Fi	2
“Raiders of the Lost Ark”	Action Adventure	2
“The Terminator”	Action Sci-Fi Thriller	2
“Back to the Future”	Adventure Comedy Sci-Fi	2
“The Fugitive”	Thriller	3
“E.T. the Extra-Terrestrial”	Children Drama Sci-Fi	3
“Groundhog Day”	Comedy Fantasy Romance	3
“Ferris Bueller’s Day Off”	Comedy	3
“Monty Python and the Holy Grail”	Adventure Comedy Fantasy	4
“Goodfellas”	Crime Drama	4
“Fargo”	Comedy Crime Drama Thriller	4

Table 1: Movielens Data. Titles, genres, and estimated cluster allocations for the 28 movies in the dataset.

Examining Figure 7, it is clear that different user clusters exhibit varying degrees of appreciation for the four identified movie genres. It is important to note that while high ratings certainly reflect a positive view of a movie, missing ratings may indicate a lack of interest. In the left column of Figure 7, we observe the rating patterns of users across the different clusters. Clusters 2 and 5 show similar rating patterns, as do Clusters 3 and 6. However, the right column, which displays the percentage of missing values for each user cluster, reveals distinct differences in the missing data. This visualization highlights the significance of considering missing entries as valuable information.

6 DISCUSSION

We introduced CO^3 , a nonparametric Bayesian method for co-clustering the rows and columns of a matrix of ordinal data, accommodating potentially informative missing entries. Our method employs matrix factorization to reduce the problem’s dimensionality, while the ordinal nature of the data is handled by introducing continuous latent variables, which facilitates model implementation. CO^3 fills a gap in the literature, as no model-based approach for co-clustering ordinal data with missing entries had previously been introduced. Consequently, in our simulation study, we compared CO^3 with a geometric approach for co-clustering that accounts for missing data, implemented in the R package `biclustermd`. The results consistently demonstrated the superior performance of

CO³ over the geometric method. Notably, CO³ proved robust even with synthetic data featuring randomly censored, and thus non-informative, missing entries. Moreover, when applied to the U.S. Senators and Movielens Data, CO³ produced interpretable and valuable results for domain experts.

The definition of CO³ relies on two independent DPs to co-cluster the rows and columns of the data matrix. Posterior simulation is achieved via a Gibbs sampling algorithm with two generalized Pólya urn steps. This structure makes CO³ highly flexible and able to infer the number of clusters in rows and columns from the data. However, this flexibility also makes posterior inference somewhat sensitive to model hyperparameters, which is a well-known limitation of models with this level of adaptability. In addition, it should be considered that Algorithm 1 does not scale well when n and p are large, primarily due to the use of a marginal algorithm, resulting from the analytical marginalization of the DPs, and the factorization applied to model the mean of continuous latent variables in (2). Addressing these limitations is essential to extend similar modeling strategies to large datasets like the Netflix Prize data¹. This may necessitate a different computational approach, with one promising option being an adaptation of the scalable multistep Monte Carlo algorithm by Ni et al. (2020). Moreover, handling extensive missing data—as is typical in the Netflix Prize data—may require an alternative modeling approach tailored to such scenarios.

¹<https://www.kaggle.com/datasets/netflix-inc/netflix-prize-data>

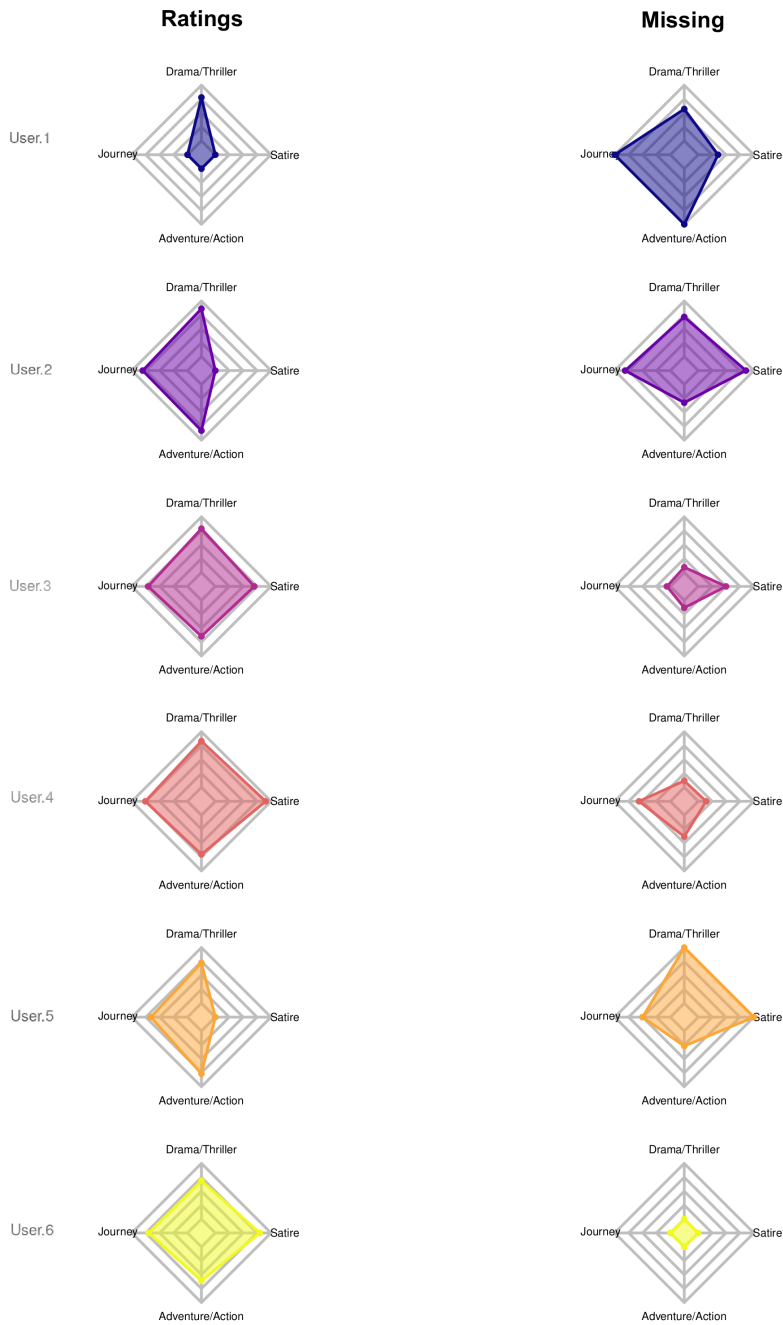


Figure 7: Movielens Data. Radar charts depicting the characterization of user clusters based on the main genres of the movies in each cluster. Ratings are displayed on the left, the percentage of missing values is shown on the right.

REFERENCES

- Albert, J. H. and S. Chib (1993). Bayesian analysis of binary and polychotomous response data. *Journal of the American statistical Association* 88(422), 669–679. [2](#), [3](#)
- Bennett, J., S. Lanning, et al. (2007). The netflix prize. In *Proceedings of KDD cup and workshop*, Volume 2007, pp. 35. New York. [1](#)
- Bhattacharya, A. and D. B. Dunson (2011). Sparse bayesian infinite factor models. *Biometrika* 98(2), 291–306. [9](#)
- Blackwell, D. and J. B. MacQueen (1973). Ferguson distributions via Pólya urn schemes. *The annals of statistics* 1(2), 353–355. [6](#)
- Boche, A., J. B. Lewis, A. Rudkin, and L. Sonnet (2018). The new Voteview.com: preserving and continuing keith poole’s infrastructure for scholars, students and observers of congress. *Public Choice* 176, 17–32. [12](#)
- Busygin, S., O. Prokopyev, and P. M. Pardalos (2008). Biclustering in data mining. *Computers & Operations Research* 35(9), 2964–2987. [2](#)
- Canale, A., R. Corradin, and B. Nipoti (2022). Importance conditional sampling for pitman–yor mixtures. *Statistics and Computing* 32(3), 40. [6](#)
- Canale, A. and D. B. Dunson (2011). Bayesian kernel mixtures for counts. *Journal of the American Statistical Association* 106(496), 1528–1539. [2](#)
- Escobar, M. D. and M. West (1995). Bayesian density estimation and inference using mixtures. *Journal of the american statistical association* 90(430), 577–588. [6](#)
- Geisser, S. and W. F. Eddy (1979). A predictive approach to model selection. *Journal of the American Statistical Association* 74(365), 153–160. [9](#)
- Hartigan, J. A. (1972). Direct clustering of a data matrix. *Journal of the american statistical association* 67(337), 123–129. [2](#)
- Irizarry, R. A. and A. Gill (2021). *dslabs: Data Science Labs*. R package version 0.7.4. [14](#)
- Ishwaran, H. and L. F. James (2001). Gibbs sampling methods for stick-breaking priors. *Journal of the American statistical Association* 96(453), 161–173. [7](#)
- Kalli, M., J. E. Griffin, and S. G. Walker (2011). Slice sampling mixture models. *Statistics and computing* 21, 93–105. [6](#)
- Kottas, A., P. Müller, and F. Quintana (2005). Nonparametric Bayesian modeling for multivariate ordinal data. *Journal of Computational and Graphical Statistics* 14(3), 610–625. [2](#), [3](#)

- Kowal, D. R. and A. Canale (2020). Simultaneous transformation and rounding (star) models for integer-valued data. *Electronic Journal of Statistics* 14(1), 1744–1772. [2](#)
- Legramanti, S., D. Durante, and D. B. Dunson (2020). Bayesian cumulative shrinkage for infinite factorizations. *Biometrika* 107(3), 745–752. [9](#)
- Meeds, E. and S. Roweis (2007). Nonparametric Bayesian biclustering. Technical report, Citeseer. [2](#)
- Ni, Y., P. Müller, M. Diesendruck, S. Williamson, Y. Zhu, and Y. Ji (2020). Scalable Bayesian nonparametric clustering and classification. *Journal of Computational and Graphical Statistics* 29(1), 53–65. [16](#)
- Papaspiliopoulos, O. and G. O. Roberts (2008). Retrospective markov chain monte carlo methods for dirichlet process hierarchical models. *Biometrika* 95(1), 169–186. [6](#)
- Rand, W. M. (1971). Objective criteria for the evaluation of clustering methods. *Journal of the American Statistical association* 66(336), 846–850. [10](#)
- Reisner, J., H. Pham, S. Olafsson, S. B. Vardeman, and J. Li (2019). biclustermd: An R Package for Biclustering with Missing values. *R J.* 11(2), 69. [2](#)
- Salakhutdinov, R. and A. Mnih (2008). Bayesian probabilistic matrix factorization using Markov chain Monte Carlo. In *Proceedings of the 25th international conference on Machine learning*, pp. 880–887. [2](#)
- Viroli, C. (2011). Finite mixtures of matrix normal distributions for classifying three-way data. *Statistics and Computing* 21, 511–522. [4](#)
- Wade, S. and Z. Ghahramani (2018). Bayesian cluster analysis: Point estimation and credible balls (with discussion). *Bayesian Analysis*. [8](#)
- Wang, P., C. Domeniconi, H. Rangwala, and K. B. Laskey (2012). Feature enriched nonparametric Bayesian co-clustering. In *Pacific-Asia Conference on Knowledge Discovery and Data Mining*, pp. 517–529. Springer. [2](#)
- Wang, P., K. B. Laskey, C. Domeniconi, and M. I. Jordan (2011). Nonparametric Bayesian co-clustering ensembles. In *Proceedings of the 2011 SIAM International Conference on Data Mining*, pp. 331–342. SIAM. [2](#)

SUPPLEMENTARY MATERIAL

This file is organized as follows. In Section A we report additional information on the full conditional distributions involved in the Gibbs sampling algorithm summarized in Algorithm 1. Section B and C provide additional results on the simulation study of Section 4 and the data analyses of Section 5, respectively,

A FULL CONDITIONAL DISTRIBUTIONS

We provide additional details on the full conditional distributions already discussed in Section 3. To this end, introducing additional notation is going to be useful. For $r = 1, 2$, we denote the r -th column of \mathbf{M}_l as $\mathbf{m}_{lr} = (m_{lr1}, \dots, m_{lrd})$; moreover, we let $v_{l s_1 s_2}$ denote the element in position (s_1, s_2) of matrix \mathbf{V}_l and $u_{l r_1 r_2}$ denote the element in position (r_1, r_2) of matrix \mathbf{U}_l .

The weights in (7) are given, up to a proportionality constant, by

$$\begin{aligned}
 \pi_{1i0} &\propto \frac{\alpha_1}{\alpha_1 + n - 1} |\tilde{\mathbf{V}}_1|^{-\frac{1}{2}} \frac{1}{\sqrt{u_{122}}} |\mathbf{V}_1|^{-\frac{1}{2}} \left| \left(\frac{1}{\sigma_1^2} \boldsymbol{\theta}_2^{(1)\top} \boldsymbol{\theta}_2^{(1)} + \tilde{\mathbf{V}}_1^{-1} \right) \right|^{-\frac{1}{2}} \\
 &\quad \times \left| \left(\frac{1}{\sigma_2^2} \boldsymbol{\theta}_2^{(2)\top} \boldsymbol{\theta}_2^{(2)} + \frac{1}{u_{122}} \mathbf{V}_1^{-1} \right) \right|^{-\frac{1}{2}} \exp \left\{ -\frac{1}{2} \text{tr} \left[\frac{1}{\sigma_1^2} \mathbf{z}_i \mathbf{z}_i^\top + \frac{1}{\sigma_2^2} \mathbf{w}_i \mathbf{w}_i^\top \right] \right\} \\
 &\quad \times \exp \left\{ -\frac{1}{2} \text{tr} \left[\tilde{\mathbf{V}}_1^{-1} \tilde{\mathbf{m}}_{11} \tilde{\mathbf{m}}_{11}^\top + \frac{1}{u_{122}} \mathbf{V}_1^{-1} \mathbf{m}_{12} \mathbf{m}_{12} \right] \right\} \\
 &\quad \times \exp \left\{ +\frac{1}{2} \text{tr} \left[\left(\frac{1}{\sigma_1^2} \boldsymbol{\theta}_2^{(1)\top} \mathbf{z}_i + \tilde{\mathbf{V}}_1^{-1} \tilde{\mathbf{m}}_{11} \right) \left(\frac{1}{\sigma_1^2} \boldsymbol{\theta}_2^{(1)\top} \mathbf{z}_i + \tilde{\mathbf{V}}_1^{-1} \tilde{\mathbf{m}}_{11} \right)^\top \left(\frac{1}{\sigma_1^2} \boldsymbol{\theta}_2^{(1)\top} \boldsymbol{\theta}_2^{(1)} + \tilde{\mathbf{V}}_1^{-1} \right)^{-1} \right] \right\} \\
 &\quad \times \exp \left\{ +\frac{1}{2} \text{tr} \left[\left(\frac{1}{\sigma_2^2} \boldsymbol{\theta}_2^{(2)\top} \mathbf{w}_i + \frac{1}{u_{122}} \mathbf{V}_1^{-1} \mathbf{m}_{12} \right) \left(\frac{1}{\sigma_2^2} \boldsymbol{\theta}_2^{(2)\top} \mathbf{w}_i + \frac{1}{u_{122}} \mathbf{V}_1^{-1} \mathbf{m}_{12} \right)^\top \left(\frac{1}{\sigma_2^2} \boldsymbol{\theta}_2^{(2)\top} \boldsymbol{\theta}_2^{(2)} + \frac{1}{u_{122}} \mathbf{V}_1^{-1} \right)^{-1} \right] \right\} \\
 \pi_{2i0} &\propto \frac{\alpha_2}{\alpha_2 + p - 1} |\tilde{\mathbf{V}}_2|^{-\frac{1}{2}} \frac{1}{\sqrt{u_{222}}} |\mathbf{V}_2|^{-\frac{1}{2}} \left| \left(\frac{1}{\sigma_1^2} \boldsymbol{\theta}_1^{(1)\top} \boldsymbol{\theta}_1^{(1)} + \tilde{\mathbf{V}}_2^{-1} \right) \right|^{-\frac{1}{2}} \left| \left(\frac{1}{\sigma_2^2} \boldsymbol{\theta}_1^{(2)\top} \boldsymbol{\theta}_1^{(2)} + \frac{1}{u_{222}} \mathbf{V}_2^{-1} \right) \right|^{-\frac{1}{2}} \\
 &\quad \times \exp \left\{ -\frac{1}{2} \text{tr} \left[\frac{1}{\sigma_1^2} \mathbf{z}_j \mathbf{z}_j^\top + \frac{1}{\sigma_2^2} \mathbf{w}_j \mathbf{w}_j^\top \right] \right\} \\
 &\quad \times \exp \left\{ -\frac{1}{2} \text{tr} \left[\tilde{\mathbf{V}}_2 \tilde{\mathbf{m}}_{21} \tilde{\mathbf{m}}_{21}^\top + \frac{1}{u_{222}} \mathbf{V}_2^{-1} \mathbf{m}_{22} \mathbf{m}_{22} \right] \right\} \\
 &\quad \times \exp \left\{ +\frac{1}{2} \text{tr} \left[\left(\frac{1}{\sigma_1^2} \boldsymbol{\theta}_1^{(1)\top} \mathbf{z}_j + \tilde{\mathbf{V}}_2^{-1} \tilde{\mathbf{m}}_{21} \right) \left(\frac{1}{\sigma_1^2} \boldsymbol{\theta}_1^{(1)\top} \mathbf{z}_j + \tilde{\mathbf{V}}_2^{-1} \tilde{\mathbf{m}}_{21} \right)^\top \left(\frac{1}{\sigma_1^2} \boldsymbol{\theta}_1^{(1)\top} \boldsymbol{\theta}_1^{(1)} + \tilde{\mathbf{V}}_2^{-1} \right)^{-1} \right] \right\} \\
 &\quad \times \exp \left\{ +\frac{1}{2} \text{tr} \left[\left(\frac{1}{\sigma_2^2} \boldsymbol{\theta}_1^{(2)\top} \mathbf{w}_j + \frac{1}{u_{222}} \mathbf{V}_2^{-1} \mathbf{m}_{22} \right) \left(\frac{1}{\sigma_2^2} \boldsymbol{\theta}_1^{(2)\top} \mathbf{w}_j + \frac{1}{u_{222}} \mathbf{V}_2^{-1} \mathbf{m}_{22} \right)^\top \left(\frac{1}{\sigma_2^2} \boldsymbol{\theta}_1^{(2)\top} \boldsymbol{\theta}_1^{(2)} + \frac{1}{u_{222}} \mathbf{V}_2^{-1} \right)^{-1} \right] \right\}.
 \end{aligned}$$

Sampling from G_{1i} in (7) is straightforward after observing that G_{1i} is the distribution of a $(d \times 2)$ -dimensional matrix \mathbf{T} , with columns \mathbf{t}_1 and \mathbf{t}_2 , for which

$$\begin{aligned}
 \mathbf{t}_1 \mid \mathbf{t}_2 &\sim \text{N}_d \left(\tilde{\mathbf{m}}_{11}, \tilde{\mathbf{V}}_1 \right) \\
 \mathbf{t}_2 &\sim \text{N}_d \left(\mathbf{m}_{12}, u_{122} \mathbf{V}_1 \right).
 \end{aligned}$$

Similarly, the distribution G_{2j} in (8) coincides with the distributions of a $(d \times 2)$ -dimensional matrix \mathbf{T} , with columns \mathbf{t}_1 and \mathbf{t}_2 , for which

$$\begin{aligned}\mathbf{t}_1 \mid \mathbf{t}_2 &\sim \text{N}_d\left(\tilde{\mathbf{m}}_{21}, \tilde{\mathbf{V}}_2\right) \\ \mathbf{t}_2 &\sim \text{N}_d\left(\mathbf{m}_{22}, u_{222} \mathbf{V}_2\right).\end{aligned}$$

Next, we show how the weights in (7) and (8) simplify when the base measures H_1 and H_2 have independent components, which is achieved, respectively, when $u_{112} = u_{121} = 0$ and $u_{212} = u_{221} = 0$.

$$\begin{aligned}\pi_{1i0} &\propto \frac{\alpha_1}{\alpha_1 + n - 1} \frac{1}{\sqrt{u_{111}}} |\mathbf{V}_1|^{-\frac{1}{2}} \frac{1}{\sqrt{u_{122}}} |\mathbf{V}_1|^{-\frac{1}{2}} \left| \left(\frac{1}{\sigma_1^2} \boldsymbol{\theta}_2^{(1)\top} \boldsymbol{\theta}_2^{(1)} + \frac{1}{u_{111}} \mathbf{V}_1^{-1} \right) \right|^{-\frac{1}{2}} \left| \left(\frac{1}{\sigma_2^2} \boldsymbol{\theta}_2^{(2)\top} \boldsymbol{\theta}_2^{(2)} + \frac{1}{u_{122}} \mathbf{V}_1^{-1} \right) \right|^{-\frac{1}{2}} \\ &\times \exp \left\{ -\frac{1}{2} \text{tr} \left[\frac{1}{\sigma_1^2} \mathbf{z}_i \mathbf{z}_i^\top + \frac{1}{\sigma_2^2} \mathbf{w}_i \mathbf{w}_i^\top \right] \right\} \\ &\times \exp \left\{ -\frac{1}{2} \text{tr} \left[\frac{1}{u_{111}} \mathbf{V}_1^{-1} \mathbf{m}_{11} \mathbf{m}_{11}^\top + \frac{1}{u_{122}} \mathbf{V}_1^{-1} \mathbf{m}_{12} \mathbf{m}_{12}^\top \right] \right\} \\ &\times \exp \left\{ +\frac{1}{2} \text{tr} \left[\left(\frac{1}{\sigma_1^2} \boldsymbol{\theta}_2^{(1)\top} \mathbf{z}_i + \frac{1}{u_{111}} \mathbf{V}_1^{-1} \mathbf{m}_{11} \right) \left(\frac{1}{\sigma_1^2} \boldsymbol{\theta}_2^{(1)\top} \mathbf{z}_i + \frac{1}{u_{111}} \mathbf{V}_1^{-1} \mathbf{m}_{11} \right)^\top \left(\frac{1}{\sigma_1^2} \boldsymbol{\theta}_2^{(1)\top} \boldsymbol{\theta}_2^{(1)} + \frac{1}{u_{111}} \mathbf{V}_1^{-1} \right)^{-1} \right] \right\} \\ &\times \exp \left\{ +\frac{1}{2} \text{tr} \left[\left(\frac{1}{\sigma_2^2} \boldsymbol{\theta}_2^{(2)\top} \mathbf{w}_i + \frac{1}{u_{122}} \mathbf{V}_1^{-1} \mathbf{m}_{12} \right) \left(\frac{1}{\sigma_2^2} \boldsymbol{\theta}_2^{(2)\top} \mathbf{w}_i + \frac{1}{u_{122}} \mathbf{V}_1^{-1} \mathbf{m}_{12} \right)^\top \left(\frac{1}{\sigma_2^2} \boldsymbol{\theta}_2^{(2)\top} \boldsymbol{\theta}_2^{(2)} + \frac{1}{u_{122}} \mathbf{V}_1^{-1} \right)^{-1} \right] \right\} \\ \pi_{2i0} &\propto \frac{\alpha_2}{\alpha_2 + p - 1} \frac{1}{\sqrt{u_{211}}} |\mathbf{V}_2|^{-\frac{1}{2}} \frac{1}{\sqrt{u_{222}}} |\mathbf{V}_2|^{-\frac{1}{2}} \left| \left(\frac{1}{\sigma_1^2} \boldsymbol{\theta}_1^{(1)\top} \boldsymbol{\theta}_1^{(1)} + \frac{1}{u_{211}} \mathbf{V}_2^{-1} \right) \right|^{-\frac{1}{2}} \left| \left(\frac{1}{\sigma_2^2} \boldsymbol{\theta}_1^{(2)\top} \boldsymbol{\theta}_1^{(2)} + \frac{1}{u_{222}} \mathbf{V}_2^{-1} \right) \right|^{-\frac{1}{2}} \\ &\times \exp \left\{ -\frac{1}{2} \text{tr} \left[\frac{1}{\sigma_1^2} \mathbf{z}_j \mathbf{z}_j^\top + \frac{1}{\sigma_2^2} \mathbf{w}_j \mathbf{w}_j^\top \right] \right\} \\ &\times \exp \left\{ -\frac{1}{2} \text{tr} \left[\frac{1}{u_{211}} \mathbf{V}_2^{-1} \mathbf{m}_{21} \mathbf{m}_{21}^\top + \frac{1}{u_{222}} \mathbf{V}_2^{-1} \mathbf{m}_{22} \mathbf{m}_{22}^\top \right] \right\} \\ &\times \exp \left\{ +\frac{1}{2} \text{tr} \left[\left(\frac{1}{\sigma_1^2} \boldsymbol{\theta}_1^{(1)\top} \mathbf{z}_j + \frac{1}{u_{211}} \mathbf{V}_2^{-1} \mathbf{m}_{21} \right) \left(\frac{1}{\sigma_1^2} \boldsymbol{\theta}_1^{(1)\top} \mathbf{z}_j + \frac{1}{u_{211}} \mathbf{V}_2^{-1} \mathbf{m}_{21} \right)^\top \left(\frac{1}{\sigma_1^2} \boldsymbol{\theta}_1^{(1)\top} \boldsymbol{\theta}_1^{(1)} + \frac{1}{u_{211}} \mathbf{V}_2^{-1} \right)^{-1} \right] \right\} \\ &\times \exp \left\{ +\frac{1}{2} \text{tr} \left[\left(\frac{1}{\sigma_2^2} \boldsymbol{\theta}_1^{(2)\top} \mathbf{w}_j + \frac{1}{u_{222}} \mathbf{V}_2^{-1} \mathbf{m}_{22} \right) \left(\frac{1}{\sigma_2^2} \boldsymbol{\theta}_1^{(2)\top} \mathbf{w}_j + \frac{1}{u_{222}} \mathbf{V}_2^{-1} \mathbf{m}_{22} \right)^\top \left(\frac{1}{\sigma_2^2} \boldsymbol{\theta}_1^{(2)\top} \boldsymbol{\theta}_1^{(2)} + \frac{1}{u_{222}} \mathbf{V}_2^{-1} \right)^{-1} \right] \right\}.\end{aligned}$$

Also sampling from G_{1i} and G_{2j} simplifies. G_{1i} is the distribution of a $(d \times 2)$ -dimensional matrix \mathbf{T} , with independent columns \mathbf{t}_1 and \mathbf{t}_2 such that

$$\begin{aligned}\mathbf{t}_1 &\sim \text{N}_d\left(\mathbf{m}_{11}, u_{111} \mathbf{V}_1\right) \\ \mathbf{t}_2 &\sim \text{N}_d\left(\mathbf{m}_{12}, u_{122} \mathbf{V}_1\right).\end{aligned}$$

Similarly, for $\mathbf{T} \sim G_{2j}$ we have

$$\begin{aligned} \mathbf{t}_1 &\sim N_d(\mathbf{m}_{21}, u_{211} \mathbf{V}_2) \\ \mathbf{t}_2 &\sim N_d(\mathbf{m}_{22}, u_{222} \mathbf{V}_2). \end{aligned}$$

We conclude this section by discussing how to implement the reshuffling step in (9). For any $\ell_1 = 1, \dots, k_n$, we let $\bar{\mathbf{z}}_{\ell_1}$ and $\bar{\mathbf{w}}_{\ell_1}$ be, respectively, the component-wise averages of the vectors \mathbf{z}_i and \mathbf{w}_i for $i \in \mathcal{C}_{\ell_1}$. By considering again the simplifying assumption $u_{112} = u_{121} = 0$, we obtain

$$\begin{aligned} \boldsymbol{\theta}_{1\ell_1}^{(1)*} \mid \dots &\stackrel{\text{ind}}{\sim} N_d\left(\left(u_{111}^{-1} \mathbf{V}_1^{-1} + n_{\ell_1} \frac{1}{\sigma_1^2} \boldsymbol{\theta}_2^{(1)} \boldsymbol{\theta}_2^{(1)\top}\right)^{-1} \left(u_{111}^{-1} \mathbf{V}_1^{-1} \mathbf{m}_{11} + n_{\ell_1} \frac{1}{\sigma_1^2} \boldsymbol{\theta}_2^{(1)} \bar{\mathbf{z}}_{\ell_1}\right), \right. \\ &\quad \left. \left(u_{111}^{-1} \mathbf{V}_1^{-1} + n_{\ell_1} \frac{1}{\sigma_1^2} \boldsymbol{\theta}_2^{(1)} \boldsymbol{\theta}_2^{(1)\top}\right)^{-1}\right) \\ \boldsymbol{\theta}_{1\ell_1}^{(2)*} \mid \dots &\stackrel{\text{ind}}{\sim} N_d\left(\left(u_{122}^{-1} \mathbf{V}_1^{-1} + n_{\ell_1} \frac{1}{\sigma_2^2} \boldsymbol{\theta}_2^{(2)} \boldsymbol{\theta}_2^{(2)\top}\right)^{-1} \left(u_{122}^{-1} \mathbf{V}_1^{-1} \mathbf{m}_{12} + n_{\ell_1} \frac{1}{\sigma_2^2} \boldsymbol{\theta}_2^{(2)} \bar{\mathbf{w}}_{\ell_1}\right), \right. \\ &\quad \left. \left(u_{122}^{-1} \mathbf{V}_1^{-1} + n_{\ell_1} \frac{1}{\sigma_2^2} \boldsymbol{\theta}_2^{(2)} \boldsymbol{\theta}_2^{(2)\top}\right)^{-1}\right) \end{aligned}$$

Similarly, for any $\ell_2 = 1, \dots, k_p$, we let $\bar{\mathbf{z}}_{\ell_2}$ and $\bar{\mathbf{w}}_{\ell_2}$ be, respectively, the component-wise averages of the vectors \mathbf{z}_j and \mathbf{w}_j for $j \in \mathcal{C}_{\ell_2}$. By considering the simplifying assumption $u_{212} = u_{221} = 0$, we obtain

$$\begin{aligned} \boldsymbol{\theta}_{2\ell_2}^{(1)*} \mid \dots &\stackrel{\text{ind}}{\sim} N_d\left(\left(u_{211}^{-1} \mathbf{V}_2^{-1} + n_{\ell_2} \frac{1}{\sigma_1^2} \boldsymbol{\theta}_1^{(1)} \boldsymbol{\theta}_1^{(1)\top}\right)^{-1} \left(u_{211}^{-1} \mathbf{V}_2^{-1} \mathbf{m}_{21} + n_{\ell_2} \frac{1}{\sigma_1^2} \boldsymbol{\theta}_1^{(1)} \bar{\mathbf{z}}_{\ell_2}\right), \right. \\ &\quad \left. \left(u_{211}^{-1} \mathbf{V}_2^{-1} + n_{\ell_2} \frac{1}{\sigma_1^2} \boldsymbol{\theta}_1^{(1)} \boldsymbol{\theta}_1^{(1)\top}\right)^{-1}\right) \\ \boldsymbol{\theta}_{2\ell_2}^{(2)*} \mid \dots &\stackrel{\text{ind}}{\sim} N_d\left(\left(u_{222}^{-1} \mathbf{V}_2^{-1} + n_{\ell_2} \frac{1}{\sigma_2^2} \boldsymbol{\theta}_1^{(2)} \boldsymbol{\theta}_1^{(2)\top}\right)^{-1} \left(u_{222}^{-1} \mathbf{V}_2^{-1} \mathbf{m}_{22} + n_{\ell_2} \frac{1}{\sigma_2^2} \boldsymbol{\theta}_1^{(2)} \bar{\mathbf{w}}_{\ell_2}\right), \right. \\ &\quad \left. \left(u_{222}^{-1} \mathbf{V}_2^{-1} + n_{\ell_2} \frac{1}{\sigma_2^2} \boldsymbol{\theta}_1^{(2)} \boldsymbol{\theta}_1^{(2)\top}\right)^{-1}\right) \end{aligned}$$

B ADDITIONAL DETAILS ON THE SIMULATION STUDY

In this section, we provide additional details on the simulation study of Section 4.

Table B1: Simulated data with ordinal observations. Estimated ARI for the marginal partitions of the rows and columns of \mathbf{Y} , along with the estimated number of clusters, \hat{k}_n and \hat{k}_p , for varying dataset sizes. Values in parentheses represent the estimated standard error. Refer to Section 4 for further details.

$n \times p$	Rows		Columns	
	ARI	\hat{k}_n	ARI	\hat{k}_p
50×50	0.880 (0.059)	2.006 (0.826)	0.932 (0.013)	2.451 (0.973)
100×100	0.895 (0.065)	3.257 (1.490)	0.961 (0.008)	2.556 (0.998)
200×200	0.957 (0.019)	3.067 (1.609)	0.970 (0.001)	3.809 (1.103)

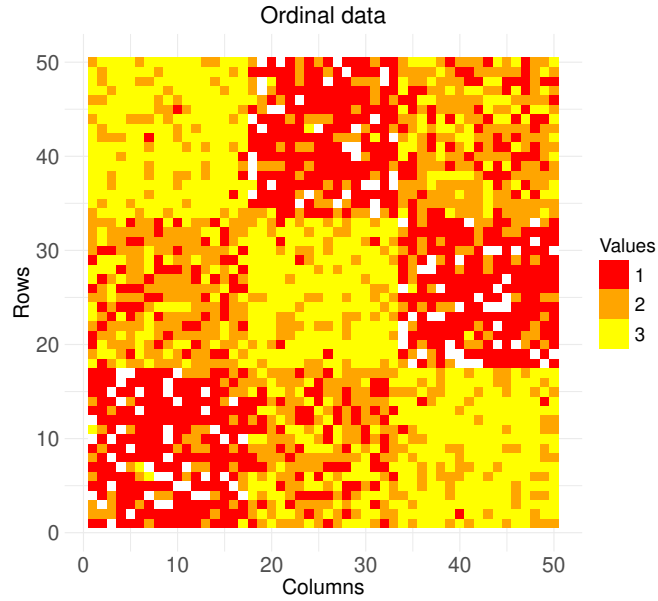


Figure B1: Graphical representation of a simulated dataset with ordinal observations. White pixels (5% of the total) indicate missing entries generated according to an informative censoring mechanism. Refer to Section 4 for further details.

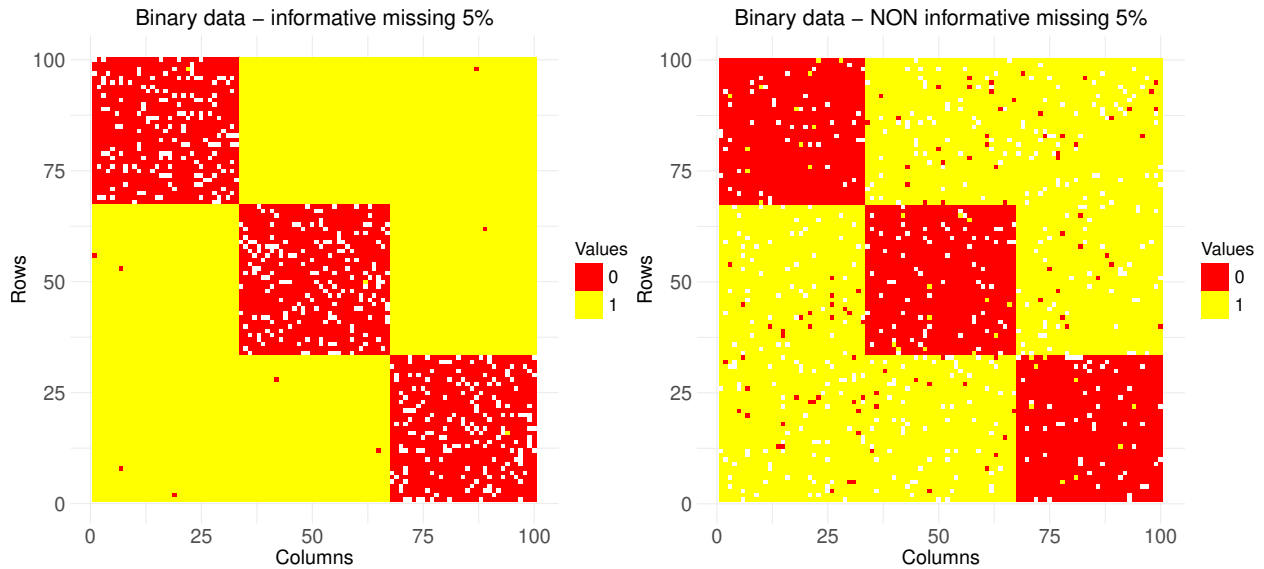


Figure B2: Graphical representation of a simulated dataset with binary observations. White pixels (5% of the total) indicate missing entries generated according to an informative censoring mechanism (left panel) or to a non-informative censoring mechanism (right panel). Refer to Section 4 for further details.

C ADDITIONAL DETAILS ON THE REAL DATA ANALYSES

In this section, we provide additional details of the analysis of datasets we presented in 5.

C.1 U.S. SENATE DATA

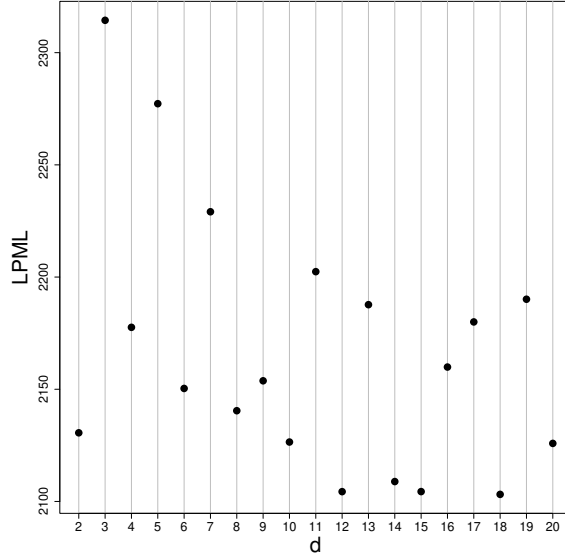


Figure C3: U.S. Senators Data. LPML as a function of the latent dimension d . Refer to Section 5.1 for further details.

Name	Party
BLUMENTHAL, Richard	Democrat
DURBIN, Richard Joseph	Democrat
FEINSTEIN, Dianne	Democrat
FISCHER, Debra (Deb)	Republican
JOHNSON, Ron	Republican
LEE, Mike	Republican
MARKEY, Edward John	Democrat
MORAN, Jerry	Republican
PAUL, Rand	Republican
RUBIO, Marco	Republican
SCHATZ, Brian Emanuel	Democrat
SCOTT, Tim	Republican
SHELBY, Richard C.	Republican
WICKER, Roger F.	Republican

Table C2: U.S. Senators Data. Names and party affiliations of the senators assigned to cluster 3 in the bottom plot of Figure 5.

C.2 MOVIELENS DATA

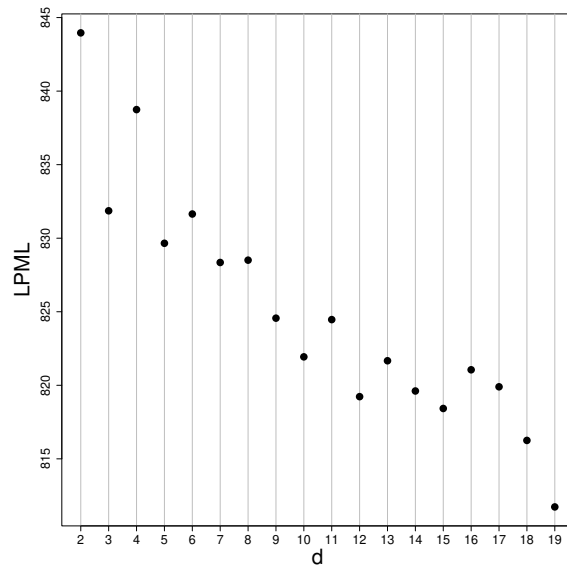


Figure C4: MovieLens Data. LPML as a function of the latent dimension d . Refer to Section 5.2 for further details.